



Sea surface
temperature patterns
in Tropical Atlantic

S. C. Kenfack et al.

Sea surface temperature patterns in Tropical Atlantic: principal component analysis and nonlinear principal component analysis

S. C. Kenfack^{1,2,5}, K. F. Mkankam², G. Alory³, Y. du Penhoat⁴,
N. M. Hounkonnou¹, D. A. Vondou², and G. N. Bawe¹

¹International Chair in Mathematical Physics and Applications, University of Abomey-Calavi, Cotonou, Benin

²Laboratory for Environmental Modeling and Atmospheric Physics, University of Yde I, Yaoundé, Cameroon

³Laboratoire d'études en Géophysique et océanographie spatiales (LEGOS), Toulouse, France

⁴IRD; LEGOS, 14 Av. Edouard Belin, 31400 Toulouse, France

⁵University of Dschang, Faculty of Science, Department of Physics, MMSL, Dschang, Cameroon

Title Page

Abstract

Introduction

Conclusions

References

Tables

Figures



Back

Close

Full Screen / Esc

Printer-friendly Version

Interactive Discussion



Received: 24 January 2014 – Accepted: 4 March 2014 – Published: 21 March 2014

Correspondence to: S. C. Kenfack (kevinsadem@yahoo.fr)

Published by Copernicus Publications on behalf of the European Geosciences Union & American Geophysical Union.

NPGD

1, 235–267, 2014

**Sea surface
temperature patterns
in Tropical Atlantic**

S. C. Kenfack et al.

Title Page

Abstract

Introduction

Conclusions

References

Tables

Figures

⏪

⏩

◀

▶

Back

Close

Full Screen / Esc

Printer-friendly Version

Interactive Discussion



Abstract

Principal Component Analysis (PCA) is one of the popular statistical methods for feature extraction. The neural network model has been performed on the PCA to obtain nonlinear principal component analysis (NLPCA), which allows the extraction of nonlinear features in the dataset missed by the PCA. NLPCA is applied to the monthly Sea Surface Temperature (SST) data from the eastern tropical Atlantic Ocean (29° W–21° E, 25° S–7° N) for the period 1982–2005. The focus is on the differences between SST inter-annual variability patterns; either extracted through traditional PCA or the NLPCA methods. The first mode of NLPCA explains 45.5% of the total variance of SST anomaly compared to 42% explained by the first PCA. Results from previous studies that detected the Atlantic cold tongue (ACT) as the main mode are confirmed. It is observed that the maximum signal in the Gulf of Guinea (GOG) is located along coastal Angola. In agreement with composite analysis, NLPCA exhibits two types of ACT, referred to as *weak* and *strong* Atlantic cold tongues. These two events are not totally symmetrical. NLPCA thus explains the results given by both PCA and composite analysis. A particular area observed along the northern boundary between 13 and 5° W vanishes in the strong ACT case and reaches maximum extension to the west in the weak ACT case. It is also observed that the original SST data correlates well with NLPCA and PCA, but with a stronger correlation on ACT area for NLPCA and southwest in the case of PCA.

1 Introduction

Thorough knowledge of our planet and its climatic variations increasingly becomes a major concern for humanity. Data collection techniques have witnessed significant progress, especially with the use of satellites for the collection of mass data; given that the density of data increases over time. Researchers have to work with more voluminous data whose management requires more original techniques.

NPGD

1, 235–267, 2014

Sea surface temperature patterns in Tropical Atlantic

S. C. Kenfack et al.

Title Page

Abstract

Introduction

Conclusions

References

Tables

Figures

⏪

⏩

◀

▶

Back

Close

Full Screen / Esc

Printer-friendly Version

Interactive Discussion



Sea surface temperature patterns in Tropical Atlantic

S. C. Kenfack et al.

Title Page

Abstract

Introduction

Conclusions

References

Tables

Figures

⏪

⏩

◀

▶

Back

Close

Full Screen / Esc

Printer-friendly Version

Interactive Discussion



Sophisticated techniques such as principal component analysis (PCA) have become indispensable in extracting essential information from voluminous data sets (Von Storch and Zwiers, 1999). The disadvantage of this conventional method is that only linear structures can be extracted from data. This limitation of determining only linear structures means that nonlinear structures are either missed or misinterpreted by these methods. Since the 1980s, models of neural networks have been increasingly documented and Kramer (1991) used this to generalize PCA and popularized its application for the extraction of nonlinear relationships in a dataset, where the PCA then extends to nonlinear principal component analysis (NLPCA). The introduction of these two techniques has become determinant in the advancement of environmental science.

Nonlinear PCA can be performed by a variety of methods, e.g. the neural network (NN) model using multi-layer perceptrons (MLP) (Kramer, 1991; Hsieh, 2004, 2007), and the kernel PCA model (Scholkopf et al., 1998). Nonlinear PCA belongs to the class of nonlinear dimensionality reduction techniques, which includes principal curves (Hastie et al., 1989), locally linear embedding (LLE) (Roweis et al., 2000) and isomap (Tenenbaum et al., 2000). A more complex technique is the Isomap, which finds a nonlinear transformation that preserves not Euclidean distances between data points, but an approximation to distances between data points as measured along geodesics in the data (Aho et al., 1983). Several extensions have since been developed to help with treating larger data sets (De Silva and Tenenbaum, 2004; Bachmann et al., 2006). In comparison, nonlinear principal component analysis (NLPCA) is an extension of the ideas of principal component analysis to settings where there is a nonlinear relationship between data variables. Here, we focus on a neural network (Hecht-Nielsen, 1995; Malthouse, 1998) based NLPCA. It is successfully applied in the fields of atmospheric and oceanic sciences (Hsieh, 2004; Monahan et al., 2003).

Many authors (e.g., Hsieh, 2001; Li et al., 2005) have studied the variations of climate in the tropical Pacific through the application of the NLPCA on the SST of this region. The subsurface thermal structure of the Pacific Ocean was also studied using the NLPCA (Tang and Hsieh, 2003). Moreover, this method of statistical analysis

Sea surface temperature patterns in Tropical Atlantic

S. C. Kenfack et al.

Title Page

Abstract

Introduction

Conclusions

References

Tables

Figures

⏪

⏩

◀

▶

Back

Close

Full Screen / Esc

Printer-friendly Version

Interactive Discussion



al., 1996). This Cold Tongue is the primary seasonal signal of sea surface temperature in the equatorial Atlantic Ocean (Merle et al., 1980; Wauthy, 1983). Within the last decades, numerous studies of climate variability in the tropical Atlantic have identified two distinct modes in the tropical Atlantic variability at inter-annual time scales (e.g., Servain and Merle, 1993; Xie et al., 1999): the equatorial mode and the meridional mode. PCA method is used by Servain et al. (1999) and the result is that the meridional mode is linked to the equatorial mode almost simultaneously. Previous study (Xie and Carton, 2004) shows that on inter-annual timescales, this equatorial mode is similar to ENSO in the Pacific. This Atlantic “El Niño” mode is most pronounced in boreal summer coinciding with the seasonal development of the equatorial cold tongue. In this paper we introduce two types of Atlantic cold tongue: *weak* and *strong* ACTs which correspond, respectively, to cold and warm anomaly in the ACT region. Some authors (Servain et al., 2003) show that the Atlantic mode is much weaker than its Pacific counterpart and according to other authors (Zebiak, 1993; Carton and Huang, 1994; Latif and Grötzner, 2000) it is the main difference between these two phenomena. Picaut et al. (1984) did a comparison between interannual variability and seasonal variability of SST in the tropical Atlantic. The result is that interannual changes in SST are largest in region where the seasonal SST signal is large.

The ocean has a strong impact on the West African climate, especially on precipitation. Many studies such as those of Ping et al. (2008) and Nnamchi et al. (2011) have attempted to assess its contribution to the establishment of the monsoon. These studies observed that the weakening of the ocean circulation in the Atlantic contributes to the slowdown of the African monsoon. Climate variability in West Africa has been associated with inter-decadal trends of sea surface temperature anomaly in the Northern and Southern Hemispheres, and also to the anomaly of sea surface temperature in the Atlantic Ocean or in the global ocean (Lamb, 1978; Palmer, 1986; Rowell et al., 1995). Moreover, modeling results (Messenger et al., 2004) show that regional sea surface temperature appears as a major factor in the seasonal and interannual precipitation of monsoon on the African continent up to 12° N. Observational study (Nicholson

and Dezfuli, 2013) shows that along the Atlantic coast, high rainfall is associated with above normal SSTs in the equatorial and South Atlantic.

Due to the effect of the Atlantic cold tongue on the West African monsoon, (Okumura and Xie, 2004; Hagos and Cook, 2008) the problem of understanding the inter-relationship between the Atlantic cold tongue and the African monsoon has remained at the center of many research endeavours. The understanding of the Atlantic cold tongue is then important to understand African climate and might better be understood using the NLPCA. Much analysis (Lamb, 1977; Lamb and Pepler, 1992; Vizy and Cook, 2001) shows that the equatorial SST in the Atlantic basin and especially in the GOG directly influences the distribution and intensity of rainfall over West Africa. Carniaux et al. (2011) shows an ACT pattern in GOG but there still is room for significant improvement. The aim of this work is to address the two questions: firstly, are the two types of ACT mentioned above symmetric? Secondly, can NLPCA show the interannual variability of SST in the tropical Atlantic?

In this paper we apply PCA and NLPCA on data from the tropical Atlantic SST. The paper is organized as follows: Sect. 2 is a brief description of the PCA and NLPCA. Section 3 describes the results of these methods on the Atlantic sea surface temperature, where we also discuss about composite analysis. The last part concludes.

2 Principal component analysis and nonlinear Principal component analysis

Linear methods of dimensionality reduction like PCA are useful tools for handling and interpreting high dimensional data. On the other hand, several nonlinear dimensionality reduction methods such as kernel PCA (kPCA), Isomap, local linear embedding (LLE) and NLPCA have been developed. Many of these nonlinear methods, including most of the differential geometry based methods and some of the neural network based methods, were originally developed in the machine learning and machine vision communities for the purpose of extracting low-dimensional information from data sets applications; such as object identification and feature tracking. Both Isomap and

Sea surface temperature patterns in Tropical Atlantic

S. C. Kenfack et al.

Title Page

Abstract

Introduction

Conclusions

References

Tables

Figures



Back

Close

Full Screen / Esc

Printer-friendly Version

Interactive Discussion



Sea surface temperature patterns in Tropical Atlantic

S. C. Kenfack et al.

Title Page

Abstract

Introduction

Conclusions

References

Tables

Figures

◀

▶

◀

▶

Back

Close

Full Screen / Esc

Printer-friendly Version

Interactive Discussion



NLPCA emanate from the PCA. Isomap is a geometrical/statistical method identified with (1) cited in the next paragraph while NLPCA (discussed later) is a Neural network method identified with (2) in the same paragraph. Isomap is the most straight way to use the geodesic distance for nonlinear projection. The goal of the Isomap (Tenenbaum et al., 2000) is to preserve the geodesics rather than the Euclidian distances. It has been broadly used in a large series of signal and image processing, pattern recognition and data analysis applications (Gómez et al., 2004). The key factor that distinguishes Isomap from NLPCA is that Isomap uses a distance function that approximates geodesic distances in the data, while the latter employs Euclidean distances in the data space. In this work we focus our attention on PCA and NLPCA.

2.1 Principal component analysis

PCA method is that which analyzes the variability of a single field (Rainfall, SST, etc.). Commonly, it is used for two objectives: (1) reducing the number of variables comprising a dataset while retaining the variability in the data and (2) identifying hidden patterns in the data, and classifying them with little loss of information. It finds the spatial patterns of variability, their time variation, and gives a measure of particular structure of each u_L pattern.

Consider a dataset $\{x_i(t)\}$, where t is the time. Assume that there is a total of N samples in t for each variable $x_i(t)$, ($i = 1, \dots, l$). We group the $\{x_i(t)\}$ into a matrix $\mathbf{x}(t)$. PCA looks for u_L which is a linear combination of the $\{x_i(t)\}$ and an associated vector, with

$$u_L = a\mathbf{x}(t) \quad (1)$$

so that $\langle \|\mathbf{x}(t) - au_L(t)\|^2 \rangle$ is minimised, and where $\langle \cdot \rangle$ denotes a sample or time mean. Here u_L is called the first principal component (PC), a time series, while a is the first eigenvector of the data covariance matrix, also called an empirical orthogonal function, (EOF), that describes a spatial pattern. From the residual, $\mathbf{x}(t) - au_L$, the second

PCA mode can similarly be extracted, and so on for higher modes. These methods have been performed using NN and become nonlinear principal component analysis (NLPCA).

2.2 Nonlinear principal component analysis

The fundamental difference between NLPCA and PCA is that NLPCA allows a nonlinear mapping from x to u_L (denoted in this part by u to make difference between NLPCA and PCA terms) whereas PCA allows only a linear mapping. A large number of specialized neural networks and learning algorithms have been proposed to perform principal component analysis (PCA) such as Isomap and NLPCA. There is no conclusive study that shows which approach is superior. The essential problem with nonlinear methods such as Isomap is that there exist few theoretical results underpinning the numerical algorithms. The network model has greater flexibility than the hierarchical model for handling complex spatial relationships.

In Fig. 1 the input column vector \mathbf{x} of length l are mapped to the neurons in the hidden layer and the transfer function q_1 maps from \mathbf{x} to the first hidden layer (the encoding layer), represented by $h^{(x)}$, a column vector of length m , with elements

$$h_k^{(x)} = q_1 \left[\left(W^{(x)} \mathbf{x} + b^{(x)} \right)_k \right], \quad (2)$$

($k = 1, \dots, m$) with the sigmoid function

$$q_1 = \tanh,$$

where $W^{(x)}$ is weight matrices and $b^{(x)}$ is bias parameter vector. The dimensions of \mathbf{x} and $h^{(x)}$ are l and m , respectively, where \mathbf{x} is the input column vector of length l , and m is the number of hidden neurons in the encoding and decoding layers for u . The neurons u is calculated from a linear combination of the hidden neurons $h^{(x)}$. A second transfer function q_2 maps the encoding layer to the bottleneck layer containing a single

Sea surface temperature patterns in Tropical Atlantic

S. C. Kenfack et al.

Title Page

Abstract

Introduction

Conclusions

References

Tables

Figures

◀

▶

◀

▶

Back

Close

Full Screen / Esc

Printer-friendly Version

Interactive Discussion



neuron, which represents the nonlinear principal component u , with

$$u = q_2 \left[W^{(x)} \cdot h^{(x)} + \bar{b}^{(x)} \right] \quad (3)$$

with identity function q_2 . These mappings are standard feed forward NNs and are capable of representing any continuous function mappings from x to u .

On the right side of Fig. 1 the top NN (a standard feed forward NN) maps u to x' in two steps:

A transfer function q_3 maps from u to the final hidden layer (the decoding layer) $h^{(u)}$,

$$h^{(u)} = q_3 \left(\left(W^{(u)} u + b^{(u)} \right)_k \right), \quad (4)$$

with $q_3 = \tanh$ and $(k = 1, \dots, m)$; followed by q_4 mapping from $h^{(u)}$ to x' , the output column vector of length l , with

$$x'_i = q_4 \left(\left(W^{(u)} h^{(u)} + \bar{b}^{(u)} \right)_i \right) \quad (5)$$

with identity function q_4 . To any given accuracy, provided large enough l and m are used to maximize by finding the optimal values of $W^{(x)}$, $b^{(x)}$, $W^{(u)}$, and $\bar{b}^{(u)}$.

The cost (Hsieh, 2001) function

$$J_1 = \langle \|x' - x\|^2 \rangle \quad (6)$$

is minimized by finding the optimal values of $W^{(u)}$, $b^{(u)}$, $W^{(u)}$, and $\bar{b}^{(u)}$. The mean square error (MSE) between the output x' and the original data x is thus minimized. Without loss of generality, we impose the constraint $\langle u \rangle = 0$, hence

$$\bar{b}^x = -\langle W^{(x)} h^{(x)} \rangle. \quad (7)$$

Sea surface temperature patterns in Tropical Atlantic

S. C. Kenfack et al.

Title Page

Abstract

Introduction

Conclusions

References

Tables

Figures

⏪

⏩

◀

▶

Back

Close

Full Screen / Esc

Printer-friendly Version

Interactive Discussion



The total number of free (weight and bias) parameters used by the NLPCA is then $2l/m + 4m + l$. Furthermore, we adopt the normalization condition that $\langle u^2 \rangle = 1$. This condition is approximately satisfied by modifying the cost function to

$$J = \langle \|x - x'\|^2 \rangle + \left(\langle u^2 \rangle - 1 \right)^2. \quad (8)$$

The choice of m , the number of hidden neurons in both the encoding and decoding layers, follows a general principle of parsimony. A larger m increases the nonlinear modeling capability of the network, but could also lead to overfitted solutions. If q_4 is the identity function, and $m = 1$, then Eq. (5) implies that all x' are linearly related to a single hidden neuron, hence there can only be a linear relation between the x' variables. For nonlinear solutions, we need to look at u . In effect, the linear relation (1) is now generalized to $u = f(x)$, where f can be any nonlinear function represented by a feed-forward NN mapping from the input layer to the bottleneck layer; and instead of $\langle \|x(t) - au_L(t)\|^2 \rangle$, $\langle \|x - g(u)\|^2 \rangle$ is minimized, where g is the general nonlinear function mapping from the bottleneck to the output layer. The residual, $x - g(u)$, can be input into the same network to extract the second NLPCA mode, and so on for the higher modes.

That the classical PCA is indeed a linear version of this NLPCA can be readily seen by replacing all the transfer functions with the identity function, thereby removing the nonlinear modeling capability of the NLPCA (Hsieh, 2001). Then the forward map to u involves only a linear combination of the original variables as in the PCA. A number of runs (mappings from u to x') used to find the solution with the smallest MSE. The NLPCA here generalizes easily to more than one hidden layer mappings, as two hidden layer mappings may outperform single hidden layer mappings in modeling complicated nonlinear functions.

We used daily Atlantic sea surface temperature (SST) data (Reynolds et al., 2007) from NOAA (National Oceanic and Atmospheric Administration). This data set is a mixture of satellite and in situ data with a spatial resolution of $0.25^\circ \times 0.25^\circ$ from 1982 to 2005 and collected between 256°S – 7°N and 29°W – 21°E . This data was combined

Sea surface temperature patterns in Tropical Atlantic

S. C. Kenfack et al.

Title Page

Abstract

Introduction

Conclusions

References

Tables

Figures

⏪

⏩

◀

▶

Back

Close

Full Screen / Esc

Printer-friendly Version

Interactive Discussion



mode in the Atlantic Ocean. NLPCA can give us information about this variability, and we may explore it in the following section.

3.2 Nonlinear principal component analysis

For SSTA data, we choose the nonlinear NLPCA model ($m = 4$) and 2 972 208 parameters which greatly exceeds the number of time points. There are still far too many spatial variables (number of point in the selected space) for this dataset to be directly analyzed by the NLPCA. To reduce the number of input variables, the SSTA data is pre-filtered by PCA and the first 3 PCs (PC1, PC2, and PC3) are used as the input to the NLPCA network. Each input variable is normalizing by subtracting its mean and then dividing by the standard deviation of the first PC (Hsieh, 2001). Scatter plots of the 3 leading principal component time series are shown by the solid black dots in Fig. 4. All four projections are shown because it is difficult to understand the structure of the NLPCA approximation from a single projection. This is particularly evident in Fig. 4c, where the curve, viewed edge-on, appears to be self-intersecting, whereas in fact the other projections demonstrate that this is not the case.

The first mode (Fig. 4) of NLPCA explains 73.5% of the variance of the given EOFs, i.e. 45.5% of the total variance of SSTA compared to 42% explained by the first PCA. The projection of NLPCA mode in the planes defined by pairing PC1, PC2, and PC3 are shown in blue in Fig. 4. Unlike the PCA, the NLPCA shows the nonlinear form in SSTA structure.

The SST anomaly manifests itself as a *Wave*-shaped curve on the non linear graph of the first nonlinear mode between the minimum and maximum value of its principal component u . The non linearity of the sinuosity observed in Fig. 4a is modest and the maximum of PC1 is smaller than the absolute value of the minimum of PC1. This shows we have a very cold event, which appears in the Atlantic region.

Figure 5 is a plot of the standardized time series of nonlinear principal component (NLPC), which bears a strong resemblance to the ACT time series (defined as the

Sea surface temperature patterns in Tropical Atlantic

S. C. Kenfack et al.

Title Page

Abstract

Introduction

Conclusions

References

Tables

Figures



Back

Close

Full Screen / Esc

Printer-friendly Version

Interactive Discussion



average SSTA over the box from 5° S to 2° N and from the coast to 20° W by Caniaux et al. (2011)). The correlation coefficient of the two series is 0.90.

Linear PCA method describes the evolution in time of a standing oscillation with fixed spatial structure and time varying amplitude. NLPCA is not so constrained, and therefore its power lies in characterizing more complex lower-dimensional structures (Monahan, 2001). The analysis of these two curves (Fig. 5) indicates that NLPCA can give information about ACT.

The most important phenomena of the GOG are active during the boreal summer, especially the Atlantic cold tongue (Xie and Carton, 2004). This Atlantic signal appears every year in the East Equatorial Atlantic (EEA) and positions itself south of the Equator with a longitudinal extent to almost 20° W, centered and located a few degrees south of the Equator in the eastern part of the basin and slightly shifted equator-ward (Caniaux et al., 2011). Since it is a seasonal phenomenon, we use Caniaux et al. (2011) formula to extract the active period for our study.

Figure 6 shows the reconstructed field of SST anomaly for some values of the first nonlinear component u . The reconstruction of the field is obtained by choosing a particular value of u associated with each of three PCs (principal components) and multiplying by the associated EOFs. Eight values of u are chosen equitably from minimum to maximum. To display the sequences of ACT (which correspond to minimum of u as Fig. 4 indicates) and the warmest SSTA (which correspond to the beginning of the ACT phase), only the eight minimum (Fig. 6) and maximum (Fig. 7) values of u are selected for each summer season (May–August) of each year. The latest is chosen for reasons given in the next section and according to Odekunle and Eludoyin (2008) results in GOG. It seems that the spatial distribution varies with each selected value of u . For the case of Fig. 6, this variation from the minimum (strong activity of Atlantic cold tongue) to maximum (low activity of Atlantic cold tongue) of the eight minimum of u shows a contrast between the north-east and southwest of 5° S. Figure 6b corresponding to 0.75 min (u) is similar to EOFa1. So, NLPCA explains variances extracted by PCA and gives more information, which is not obvious by analysis with the PCA.

Sea surface temperature patterns in Tropical Atlantic

S. C. Kenfack et al.

Title Page

Abstract

Introduction

Conclusions

References

Tables

Figures

⏪

⏩

◀

▶

Back

Close

Full Screen / Esc

Printer-friendly Version

Interactive Discussion



Sea surface temperature patterns in Tropical Atlantic

S. C. Kenfack et al.

Title Page

Abstract

Introduction

Conclusions

References

Tables

Figures

⏪

⏩

◀

▶

Back

Close

Full Screen / Esc

Printer-friendly Version

Interactive Discussion



Fig. 7 which is obvious because it is the early phase of the development of ACT. We observe that the variance is more positive than the one observed in Fig. 6. In particular, cold events described by NLPCA mode 1 displays the strongest anomalies near the Angola coast in the south region centered around 17° W, which increases from the south to the north. Odekunle and Eludoyin (2008) shows that the Cameroon coastal border is warmer and in (Fig. 6) we observed that this warmer region on the west side occurs when ACT is at its maximum and it is seen that the active upwelling are located in two regions: the Angolan and the Ghanaian coasts. Some results (Reason and Rouault, 2006) suggest that the Angolan coast variability can strongly have an effect surrounding area climate and that the strongest relationships exist between SST in the Angola-Benguela Frontal Zone area and rainfall over the region 5° W– 5° E, 5 – 10° N.

The spatial distribution is best described (Fig. 6) by NLPCA than PCA, and the variance may be represented by these first NLPCA modes. This mode is the resultant of two linear modes of the PCA. The asymmetry of SSTA in the evolution of NLPCA mode 1 is modest; the warm event is lightly southwards than the cold event.

Monahan (2001) observed for the results in the Pacific Ocean that the NLPCA mode 1 is primarily a mixture of PCA modes 1 and 2. It is the same in this study. Figure 6 shows strong ACT interchange with Ghana upwelling and also its activity from West to East. Caniaux et al. (2011) observed, Fig. 6a and h exhibit, respectively, small and big cooling area and show that cooling is not proportional to surface area. The largest SST anomalies are located in Angola coast during strong and weak average ACT events. ACT spreads slowly, but increases, and decreases, towards the west and east, respectively. It is more active in Eastwards than westwards. Cold activity of ACT is more intense than warm one; this means that strong ACT is more active than weak one. Comparison between Figs. 6a–h and 7a–h shows that the type (strong or weak) of ACT depends on SSTA activity before its formation. We observe that strong ACT corresponds to cold activity before its formation and weak ACT is associated to warm activity before the ACT development. But observing Figs. 6g and 7g, we may conclude

that it cannot be generalized. This means that the ACT activity is not totally dependent on its surface.

In Fig. 6c, d, and h is observed a particular event occurring in a circle along the equator between 13 and 5° W. Its surface area increases from strong to weak ACT; with maximum for weak and minimum for strong ACTs, respectively. We may also observe that the maximum is displaced more to the West (from the coast) than the minimum. Some authors (Hastenrath and Lamb, 1977; Houghton, 1983) recently showed that cold water appears as a narrow band along the northern boundary between 2° E and 8° W. NLPCA exhibits the same result with special information on the spatial variability of this space. The magnitude of this area is more important during weak ACT.

3.3 Composite analysis

Figure 8a is a composite analysis of May-June-July-August (MJJA) average SSTA for the years in which the SST index (mentioned above, Caniaux et al., 2011) is greater than one standard deviation above the long-term mean. Figure 8b is the same for the MJJA for which SST index is less than one standard deviation below the long-term mean. This averaging period was used for the composites because MJJA displays the period which the surface area at less than 25°C is greater than the empirical threshold surface area at $0.40 \times 10^6 \text{ km}^2$ (Caniaux et al., 2011). These two maps correspond to the SSTA patterns of an average warm and cold ACT event, respectively. The spatial asymmetry between cold and warm events of ACT observed in NLPCA mode 1 is manifests in composite analysis. These two maps correspond to the SSTA patterns of an average *weak* and *strong* ACT, respectively.

Figure 8a and b, respectively, bears a strong resemblance to Fig. 6h and a; and are strongly similar to EOFa1. This means that EOF1a exhibit strong ACT. It is more explicit in the first NLPCA mode 1, which shows both strong and weak ACTs.

Note that, consistent with the maps corresponding to the 1D NLPCA (Fig. 6), the largest SSTA tend to be located in the Angola coast during the average strong and

Title Page

Abstract

Introduction

Conclusions

References

Tables

Figures

◀

▶

◀

▶

Back

Close

Full Screen / Esc

Printer-friendly Version

Interactive Discussion



weak ACT events. The spatial correlation between the two maps is -0.98 . This confirms the symmetry between the warm and cold ACT events.

A final comparison of the 1D NLPCA and 1D PCA approximations is given in Fig. 9, which shows, respectively, maps of the pointwise correlation between the original SSTA data and the 1D PCA approximation, and of the pointwise correlation between SSTA and the 1D NLPCA approximation (Fig. 9). The two approximations are equally well correlated with the original data over the central band of the Atlantic Ocean, where the NLPCA correlations are somewhat higher than those of the PCA approximation, except in the Southwest part of the Ocean. In the Angolan region and in the ACT the 1D NLPCA approximation displays a greater fidelity to the original data, as determined by the pointwise correlation, than does the 1D PCA approximation. This demonstrates the better capacity of NLPCA in representing SST data than the PCA.

We observe that NLPCA represents better ACT surface on the Angolan coast than the PCA. However strong correlation in Fig. 9 centered at around 15° W in Southern of ACT surface shows the ability of PCA to reproduce SSTA data in this region. Therefore, the NLPCA and PCA are complementary. In this mode, these two statistical tools do not strongly represent SSTA data on the Namibia and along Cameroon-Liberia coasts as the tropical Atlantic Ocean.

4 Conclusions

We have investigated the application of linear PCA and nonlinear generalization of PCA, to tropical Atlantic SST. It was found that a NLPCA mode 1 explains 45.5% of the total variance in the SST field, in contrast to 42% for the first PCA mode. The NLPC mode 1 described the ACT variability which is exhibited in the time series u (Fig. 5) and the sequence of spatial maps (Fig. 6). PCA mode 1 also characterizes average ACT variability, but only as a standing oscillation, so it is unable to evaluate the asymmetry in spatial pattern between average warm and cold events manifested in the 1D NLPCA. Compared to PCA, NLPCA can better point out the two type of ACT:

Sea surface temperature patterns in Tropical Atlantic

S. C. Kenfack et al.

Title Page

Abstract

Introduction

Conclusions

References

Tables

Figures

◀

▶

◀

▶

Back

Close

Full Screen / Esc

Printer-friendly Version

Interactive Discussion



Sea surface temperature patterns in Tropical Atlantic

S. C. Kenfack et al.

Title Page

Abstract

Introduction

Conclusions

References

Tables

Figures

⏪

⏩

◀

▶

Back

Close

Full Screen / Esc

Printer-friendly Version

Interactive Discussion



the *strong* and *weak*. NLPCA can better represent all the SST data than PCA. We note that non linearity in spatial variation of SSTA is modest in Atlantic Ocean in contrast to the Ocean Pacific Ocean. Both warm and cold surface events develop regularly in the same specific region along the coast of Angola and Namibia. The NLPCA indicates that Angola upwelling has a strong relation with Atlantic cold tongue. The less intense the Angola upwelling, the smaller the surface area of Atlantic cold tongue.

Apart from a weakly nonlinear 1D NLPCA corresponding to variability between average strong ACT and average weak ACT events, the results obtained also show that the robust low-dimensional structure of the SSTA data appears along the equator between 13 and 5° W. It has been observed that in summer the interannual variability of SST is more active near the Angolan coast than the other parts of GOG. The Atlantic equatorial mode which is similar to El Nino/Southern Oscillation (ENSO) in the Pacific Ocean has been recognized and it is shown that it is less linear than the latter. Detailed analysis shows that NLPCA represents better ACT surface and Angolan coast than PCA although the two methods remain important to analyse voluminous data. It is seen that the activity of ACT is independent of its surface. Future analysis is needed to further explore the relationship between Angola upwelling and ACT. It will be equally important to study West African monsoon rainfall using NLPCA and the intended implications of SST for the spatio-temporal variability of precipitation over West Africa.

Acknowledgements. This work was supported by the Mwalimu Nyerere African Union Scholarship Scheme (MNAUSS). The authors would like to thank Hsieh W. William for his guidance and suggestion on an early draft of the paper.

References

- Aho, A. V., Hopcroft, J. E., and Ullman, J. D.: Data Structures and Algorithms, Addison-Wesley, 1983. 238
- Aires, F. and Ché din, A.: Independent component analysis of multivariate time series: Application to the tropical SST variability, *J. Geophys. Res.*, 105, 437–455, 2000. 239

Sea surface temperature patterns in Tropical Atlantic

S. C. Kenfack et al.

Title Page

Abstract

Introduction

Conclusions

References

Tables

Figures

◀

▶

◀

▶

Back

Close

Full Screen / Esc

Printer-friendly Version

Interactive Discussion



- Bachmann, C. M., Ainsworth, T. L., and Fusina, R. A.: Improved manifold coordinate representations of large-scale hyperspectral scenes, *IEEE T. Geosci. Remote*, 44, 2786–2803, 2006. 238
- Caniaux, G., Giordani, H., Redelsperger, J.-L., Guichard, F., Key, E., and Wade, M.: Coupling between the Atlantic cold tongue and the West African monsoon in boreal spring and summer, *J. Geophys. Res.*, 116, C04003, doi:10.1029/2010JC006570, 2011. 241, 248, 250, 251
- Carton, J. A. and Huang, B.: Warm events in the tropical Atlantic, *J. Phys. Oceanogr.*, 24, 888–903, 1994. 240
- Carton, J. A., Cao, X., Giese, B., and Da Silva, A. M.: Decadal and interannual sst variability in the tropical atlantic, *J. Phys. Oceanogr.*, 26, 1165–1175, 1996. 239
- Chen, H., Yin, B., Fang, G., and Wang, Y.: Comparison of nonlinear and linear PCA on surface wind, surface height, and SST in the South China Sea, *Chin. J. Oceanol. Limnol.*, 28, 981–989, 2010. 239
- Constantin, A.: Principal component analysis of sea surface temperature in the north Atlantic ocean, *Int. J. Mod. Phys. C*, 20, 1789–1802, 2009. 239
- De Silva, V. and Tenenbaum, J. B.: Sparse multidimensional scaling using landmark points, *Stanford Mathematics Technical Report*, 41 pp., 2004. 238
- Everson, R., Cornillon, P., Sirovich, L., and Webber, A.: An empirical eigenfunction analysis of sea surface temperature in the western North Atlantic, *Journal of Geophysical Oceanography*, 27, 468–479, 1997. 239
- Gómez, A. J., Zhou, C. S., Timmermann, A., and Kurths, J.: Nonlinear dimensionality reduction in climate data, *Nonlin. Processes Geophys.*, 11, 393–398, doi:10.5194/npg-11-393-2004, 2004. 242
- Hagos, S. M. and Cook, K. H.: Development of a coupled regional model and its application to the study of interactions between the West African monsoon and the eastern tropical Atlantic ocean, *J. Climate*, 18, 4993–5010, 2008. 241
- Hastenrath, S. and Lamb, P. J.: *Climatic Atlas of the Tropical Atlantic and Eastern Pacific Oceans*, The University of Wisconsin Press, Madison, 112 pp., 1977. 251
- Hastie, T. and Stuetzle, W.: Principal curves, *J. Am. Stat. Assoc.*, 84, 502–516, 1989. 238
- Hecht-Nielsen, R.: Replicator neural networks for universal optimal source coding, *Science*, 269, 1860–1863, 1995. 238

Sea surface temperature patterns in Tropical Atlantic

S. C. Kenfack et al.

Title Page

Abstract

Introduction

Conclusions

References

Tables

Figures

⏪

⏩

◀

▶

Back

Close

Full Screen / Esc

Printer-friendly Version

Interactive Discussion



- Hirst, A. C. and Hastenrath, S.: Atmosphere-ocean mechanisms of climate anomalies in the Angola-tropical Atlantic sector, *J. Phys. Oceanogr.*, 13, 1146–1157, 1983. 239, 249
- Houghton, R. W.: Seasonal variations of the subsurface thermal structure in the Gulf of Guinea, *J. Phys. Oceanogr.*, 13, 2070–2081, 1983. 251
- 5 Hsieh, W. W.: Non linear principal component analysis by neural networks, *Tellus*, 53, 599–615, 2001. 238, 244, 245, 247
- Hsieh, W. W.: nonlinear multivariate and time series analysis by neural network methods, *Rev. Geophys.*, 42, RG1003, doi:10.1029/2002RG000112, 2004. 238, 239
- Hsieh, W. W.: Nonlinear principal component analysis of noisy data, *Neural Networks*, 20, 434–443, 2007. 238, 239
- 10 Kramer, M. A.: Non-linear principal component analysis using auto associative neural networks, *AIChE J.*, 37, 233–243, 1991. 238
- Lamb, P. J.: Largescale tropical atlantic surface circulation patterns associated with sub-saharan weather anomalies, *Tellus*, 30, 240–251, 1977. 241
- 15 Lamb, P. J.: Large-scale tropical Atlantic surface circulation patterns associated with sub-Saharan weather anomalies, *Tellus*, 30, 240–251, 1978. 240
- Lamb, P. J. and Pepler, R. A.: Further case studies of tropical atlantic surface atmospheric and oceanic patterns associated with sub-saharan drought, *J. Climate*, 5, 472–488, 1992. 241
- Latif, M. and Grötzner, A.: The equatorial Atlantic oscillation and its response to ENSO, *Clim. Dynam.*, 16, 213–218, 2000. 240
- 20 Li, T. and Philander, S. G. H.: On the seasonal cycle of the equatorial Atlantic Ocean, *J. Climate*, 10, 813–817, 1997. 239
- Li, S., Hsieh, W. W., and Wu, A.: Hybrid coupled modeling of the tropical Pacific using neural networks, *J. Geophys. Res.*, 110, C09024, doi:10.1029/2004JC002595, 2005. 238
- 25 Malthouse, E. C.: Limitations of nonlinear pca as performed with generic neural networks, *IEEE T. Neural Networ.*, 9, 165–173, 1998. 238
- Merle, J., Fieux, M., and Hisard, P.: Annual signal and interannual anomalies of sea surface temperature in the eastern equatorial Atlantic Ocean, *Deep-Sea Res.*, 26, 77–101, 1980. 239, 240
- 30 Messenger, C., Gallee, H., and Brasseur, O.: Precipitation sensitivity to regional SST in a regional climate simulation during the West African monsoon for two dry years, *Clim. Dynam.*, 22, 249–266, 2004. 240

Sea surface temperature patterns in Tropical Atlantic

S. C. Kenfack et al.

Title Page

Abstract

Introduction

Conclusions

References

Tables

Figures

◀

▶

◀

▶

Back

Close

Full Screen / Esc

Printer-friendly Version

Interactive Discussion



- Monahan, A. H.: Nonlinear principal component analysis: Tropical Indo-Pacific sea surface temperature and sea level pressure, *J. Climate*, 14, 219–233, 2001. 239, 248, 250
- Monahan, A. H., Fyfe, J. C., and Pandolfo, L.: The vertical structure of wintertime climate regimes of the northern hemisphere extratropical atmosphere, *J. Climate*, 16, 2005–2021, 2003. 238
- Nicholson, S. E. and Dezfuli, A. K.: The Relationship of Rainfall Variability in Western Equatorial Africa to the Tropical Oceans and Atmospheric Circulation. Part I: The Boreal Spring, *J. Climate*, 26, 45–65, 2013. 240
- Nnamchi, H. C. and Jianping, L.: Influence of the South Atlantic Ocean Dipole on West African Summer Precipitation, *J. Climate*, 24, 1184–1197, 2011. 240
- Odekunle, T. O. and Eludoyin, A. O.: Sea surface temperature patterns in the Gulf of Guinea: their implications for the spatio-temporal variability of precipitation in West Africa, *Int. J. Climatol.* 28, 1507–1517, 2008. 248, 250
- Okumura, Y. and Xie, S. P.: Interaction of the Atlantic equatorial Cold Tongue and the African Monsoon, *J. Climate*, 17, 3589–3602, 2004. 241
- Palmer, T. N.: The influence of the Atlantic, Pacific and Indian Oceans on Sahel rainfall, *Nature*, 322, 251–253, 1986. 240
- Philander, S. G. H.: Unusual conditions in the tropical Atlantic Ocean in 1984, *Nature*, 322, 236–238, 1986. 239
- Picaut, J., Servain, J., Busalacchi, A. J., and Seva, M.: Interannual Variability Versus Seasonal variability in the tropical Atlantic, *Geophys. Res. Lett.*, 11, 787–790, 1984. 240
- Ping, C., Rong, Z., Hazeleger, W., Wen, C., Wan, X., Ji, L., Haarsma, R. J., Breugem, W.-P., and Seidel, H.: Oceanic link between abrupt changes in the North Atlantic Ocean and the African monsoon, *Nat. Geosci.*, 1, 444–448, 2008. 240
- Reason, C. J. C. and Rouault, M.: Sea surface temperature variability in the tropical south Atlantic Ocean and West African rainfall, *Geophys. Res. Lett.*, 33, L21705, doi:10.1029/2006/GL027145, 2006. 250
- Reynolds, R. W., Smith, T. S., Liu, C., Chelton, D. B., Casey, K. S., and Schlax, M. G.: Daily High-Resolution-Blended Analyses for Sea Surface Temperature, *J. Climate*, 20, 5473–5496, 2007. 245
- Rouault, M., Florenchie, P., Fauchereau, N., and Reason, C. J. C.: South east Atlantic warm events and southern African rainfall, *Geophys. Res. Lett.*, 30, 8009, doi:10.1029/2002GL014840, 2003. 249

Sea surface temperature patterns in Tropical Atlantic

S. C. Kenfack et al.

Title Page

Abstract

Introduction

Conclusions

References

Tables

Figures

◀

▶

◀

▶

Back

Close

Full Screen / Esc

Printer-friendly Version

Interactive Discussion



- Roweis, S. T. and Saul, L. K.: Nonlinear dimensionality reduction by locally linear embedding, *Science*, 290, 2323–2326, 2000. 238
- Rowell, D. P., Folland, C. K., Maskell, K., and Ward, M. N.: Variability of summer rainfall over tropical North Africa (1906–92): observations and modeling, *Q. J. Roy. Meteor. Soc.*, 121, 669–704, 1995. 240
- Scholkopf, B., Smola, A., and Muller, K.-R.: Nonlinear component analysis as a kernel eigenvalue problem, *Neural Comput.*, 10, 1299–1319, 1998. 238
- Servain, J. and Merle, J.: Interannual climate variations over the tropical Atlantic Ocean, in: *Prediction of Interannual Climate Variations*, edited by: Shukla, J., Springer-Verlag, Berlin, NATO ASI Series, 16, 153–171, 1993. 240
- Servain, J., Picaut, J., and Merle, J.: Evidence of remote forcing in the equatorial Atlantic Ocean, *J. Phys. Oceanogr.*, 12, 457–463, 1982. 239
- Servain, J., Wainer, I., McCreary, J. P., and Dessier, A.: Relationship between the Equatorial and meridional modes of climatic variability in the tropical Atlantic, *Geophys. Res. Lett.*, 26, 485–488, 1999. 240
- Servain, J., Clauzet, G., and Wainer, I. C.: Modes of tropical Atlantic climate variability observed by PIRATA, *Geophys. Res. Lett.*, 30, 8003, doi:10.1029/2002GL015124, 2003. 240
- Tang, Y. and Hsieh, W. W.: Nonlinear modes of decadal and interannual variability of the subsurface thermal structure in the Pacific Ocean, *J. Geophys. Res.*, 108, 3084, doi:10.1029/2001JC001236, 2003. 238
- Tenenbaum, J. B., de Silva, V., and Langford, J. C.: A global geometric framework for nonlinear dimensionality reduction, *Science*, 290, 2319–2323, 2000. 238, 242
- Vizy, E. K. and Cook, K. H.: Mechanisms by which gulf of guinea and eastern north atlantic sea surface temperature anomalies can influence african rainfall, *J. Climate*, 14, 795–821, 2001. 241
- Von Storch, H. and Zwiers, F. W.: *Statistical Analysis in Climate Research*, Cambridge Univ. Press, New York, 484 pp., 1999. 238
- Wauthy, B.: *Introduction a la climatologie du Golfe de Guinée*, *Océanogr. Trop.*, 18, 103–138, 1983 (in French). 240
- Wilson-Diaz, D., Mariano, A. J., Evans, R. H., and Luther, M. E.: A principal component analysis of sea-surface temperature in the Arabian Sea, *Deep-Sea Res. Pt. II*, 48, 1097–1114, 2001. 239

- Xie, S.-P. and Carton, J. A.: Tropical Atlantic Variability: Patterns, Mechanisms, and Impacts, AGU, Washington, D.C., Geophysical Monograph, 147, 121–142, 2004. 239, 240, 248, 249
- Xie, S.-P., Tanimoto, Y., Noguchi, H., and Matsuno, T.: How and why climate variability differs between the tropical Atlantic and Pacific, Geophys. Res. Lett., 26, 1609–1612, 1999. 240
- 5 Zebiak, S. E.: Air-sea interaction in the equatorial Atlantic region, J. Climate, 6, 1567–1586. 1993. 240

**Sea surface
temperature patterns
in Tropical Atlantic**

S. C. Kenfack et al.

Title Page

Abstract

Introduction

Conclusions

References

Tables

Figures



Back

Close

Full Screen / Esc

Printer-friendly Version

Interactive Discussion



Sea surface temperature patterns in Tropical Atlantic

S. C. Kenfack et al.

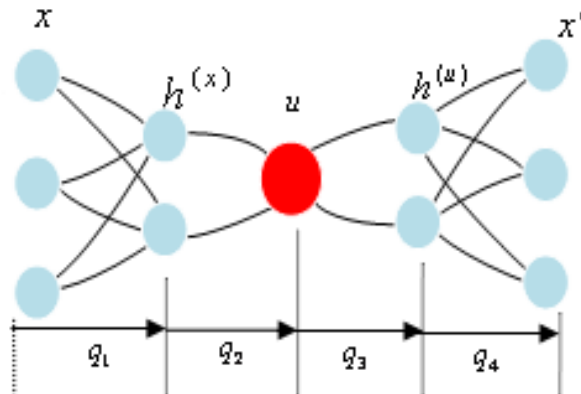


Fig. 1. The NN model for calculating nonlinear PCA. There are 3 “hidden” layers of variables or “neurons” (denoted by circles) sandwiched between the input layer x on the left and the output layer x' on the right. Next to the input layer is the encoding layer, followed by the “bottleneck” layer (with a single neuron u for NLPCA), which is then followed by the decoding layer. q_1 , q_2 , q_3 , and q_4 are the transfer functions.

Title Page

Abstract

Introduction

Conclusions

References

Tables

Figures

◀

▶

◀

▶

Back

Close

Full Screen / Esc

Printer-friendly Version

Interactive Discussion



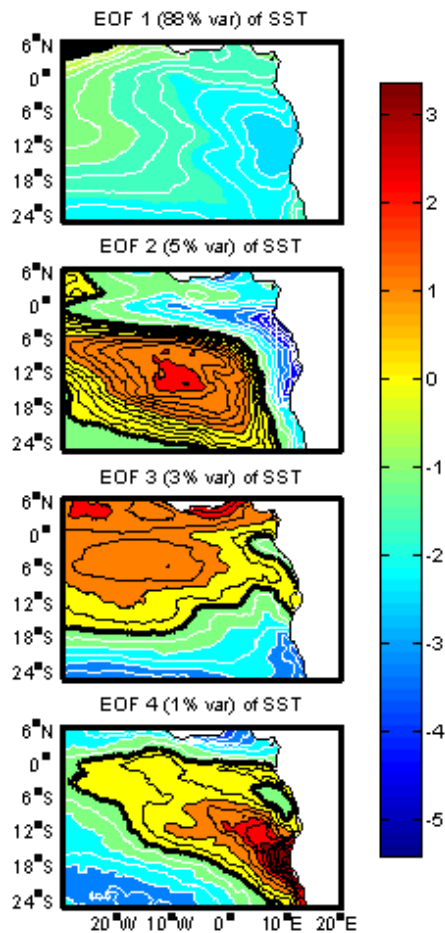


Fig. 2. Spatial patterns of the first EOF modes of SST. Negative contours are white lines. Zero line is bold black and positive contours are black. The contour interval is 0.01.

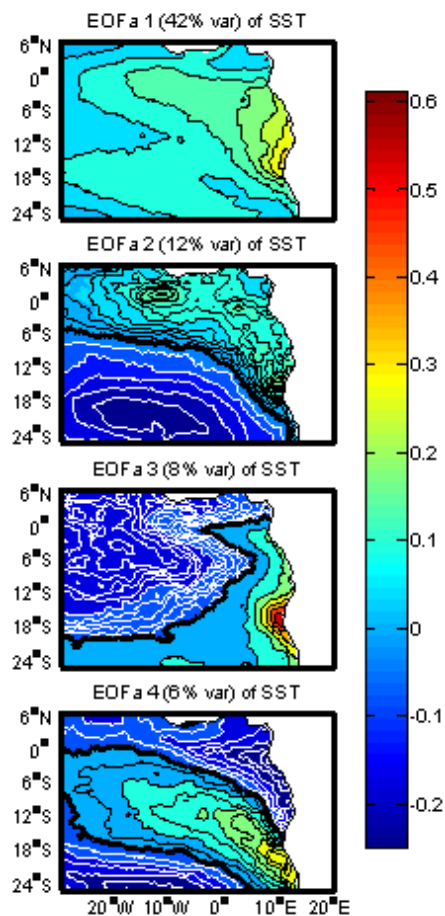


Fig. 3. As in Fig. 2 but for SSTA.

Sea surface temperature patterns in Tropical Atlantic

S. C. Kenfack et al.

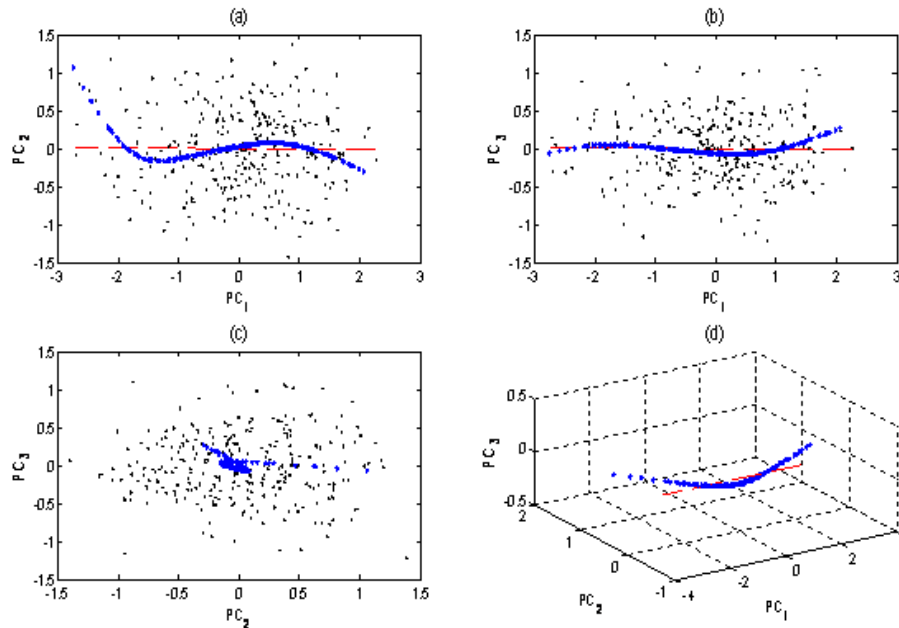


Fig. 4. Scatter plot of the sea surface temperature (SST) anomaly (SSTA) data (shown as dot) in the principal component (PC1, PC2, and PC3) plane. The first principal component analysis (PCA) eigenvector is oriented along the horizontal line. The first mode NLPKA approximation to the data is shown by the blue circles, which traced out a *Wave*-shaped curve.

[Title Page](#)[Abstract](#)[Introduction](#)[Conclusions](#)[References](#)[Tables](#)[Figures](#)[◀](#)[▶](#)[◀](#)[▶](#)[Back](#)[Close](#)[Full Screen / Esc](#)[Printer-friendly Version](#)[Interactive Discussion](#)

Sea surface temperature patterns in Tropical Atlantic

S. C. Kenfack et al.

Title Page

Abstract

Introduction

Conclusions

References

Tables

Figures



Back

Close

Full Screen / Esc

Printer-friendly Version

Interactive Discussion

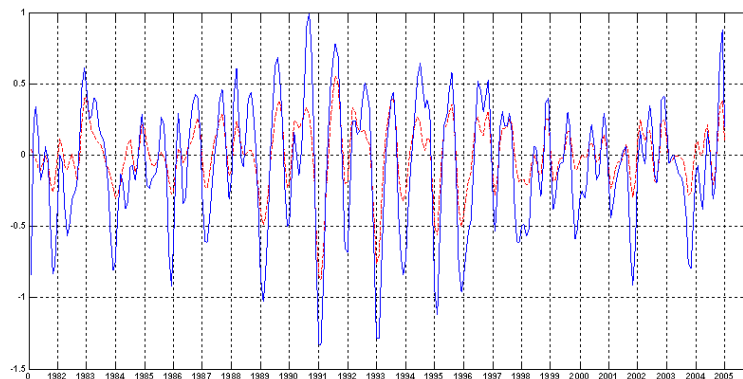


Fig. 5. Plot of NLPC1, the time series associated with SSTA NLPCA mode 1 (blue line) and the normalized ACT index (red dashed line).

Sea surface temperature patterns in Tropical Atlantic

S. C. Kenfack et al.

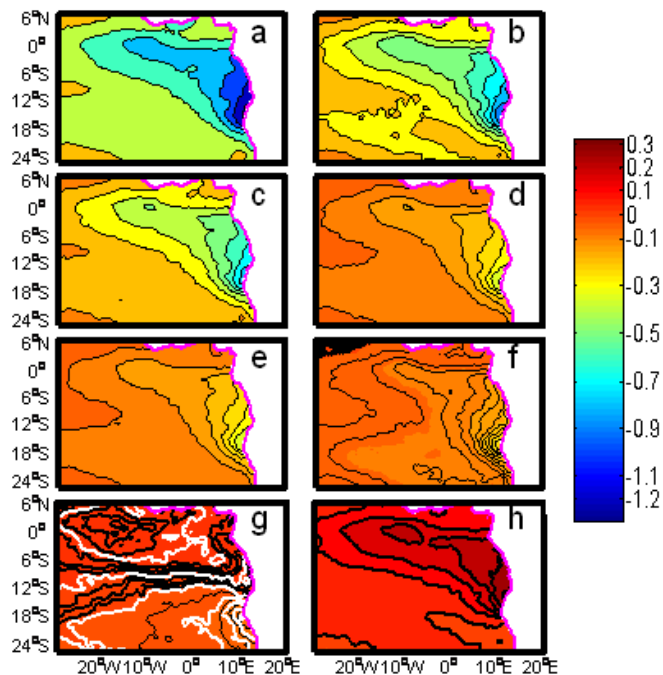


Fig. 6. The SST anomaly pattern (in $^{\circ}\text{C}$) of the NLPCA as the minimum of NLPC u between May and August for each year of the first NLPCA mode. Considering just the eight minimum mentioned above, the anomaly pattern of the first NLPCA mode varies from **(a)** its minimum (*strong* Atlantic cold tongue), to **(b)** three-quarter its minimum, to **(c)** half its minimum, to **(d)** quarter of its minimum, to **(e)** quarter its maximum, to **(f)** half its maximum, to **(g)** three-quarter its maximum and **(h)** its maximum (*weak* Atlantic cold tongue). Zero contours are white lines. Positive contour is bold black line and negative contours are black.

Sea surface temperature patterns in Tropical Atlantic

S. C. Kenfack et al.

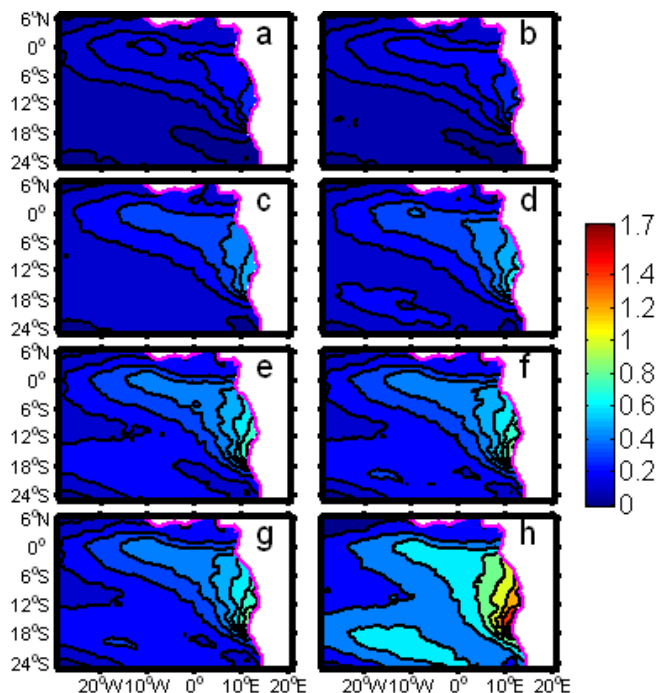


Fig. 7. The SST anomaly pattern (in °C) of the NLPCA as the maximum of NLPC u between May and August for each year of the first NLPCA mode. From the eight maxim values of u , the anomaly pattern of the first NLPCA mode varies from **(a)** its minimum (strong starting phase of ACT), to **(b)** three-quarter its minimum, to **(c)** half its minimum, to **(d)** quarter its minimum, to **(e)** quarter its maximum, to **(f)** half its maximum, to **(g)** three-quarter its maximum and **(h)** its maximum (weak starting phase of ACT).

Sea surface temperature patterns in Tropical Atlantic

S. C. Kenfack et al.

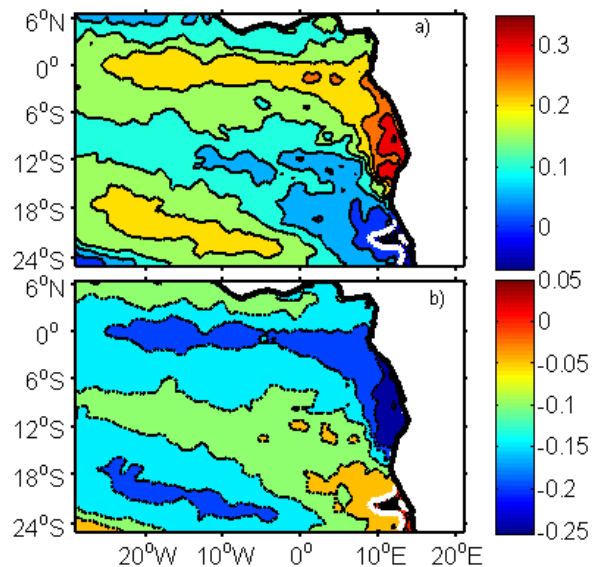


Fig. 8. Composite maps for average **(a)** warm ACT and **(b)** cold ACT events in °C unit.

[Title Page](#)[Abstract](#)[Introduction](#)[Conclusions](#)[References](#)[Tables](#)[Figures](#)[◀](#)[▶](#)[◀](#)[▶](#)[Back](#)[Close](#)[Full Screen / Esc](#)[Printer-friendly Version](#)[Interactive Discussion](#)

Sea surface temperature patterns in Tropical Atlantic

S. C. Kenfack et al.

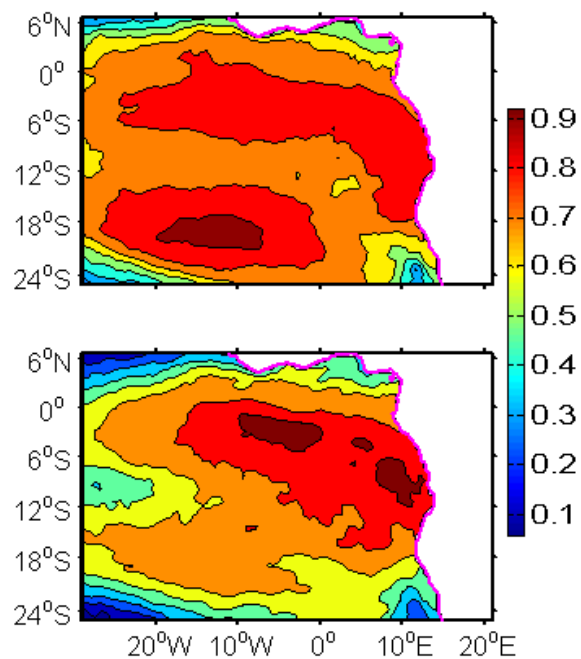


Fig. 9. Maps of pointwise correlation coefficients between observed SSTA and **(a)** 1D PCA approximation and **(b)** 1D NLPCA approximation.

[Title Page](#)[Abstract](#)[Introduction](#)[Conclusions](#)[References](#)[Tables](#)[Figures](#)[◀](#)[▶](#)[◀](#)[▶](#)[Back](#)[Close](#)[Full Screen / Esc](#)[Printer-friendly Version](#)[Interactive Discussion](#)